JOURNAL OF THE AMERICAN WATER RESOURCES ASSOCIATION

Vol. 49, No. 3

AMERICAN WATER RESOURCES ASSOCIATION

June 2013

ESTIMATING ANNUAL GROUNDWATER EVAPOTRANSPIRATION FROM PHREATOPHYTES IN THE GREAT BASIN USING LANDSAT AND FLUX TOWER MEASUREMENTS[1]

Jordan P. Beamer, Justin L. Huntington, Charles G. Morton, and Greg M. Pohll[2]

ABSTRACT: Escalating concerns about water supplies in the Great Basin have prompted numerous water budget studies focused on groundwater recharge and discharge. For many hydrographic areas (HAs) in the Great Basin, most of the recharge is discharged by bare soil evaporation and evapotranspiration (ET) from phreatophyte vegetation. Estimating recharge from precipitation in a given HA is difficult and often has significant uncertainty, therefore it is often quantified by estimating the natural discharge. As such, remote sensing applications for spatially distributing flux tower estimates of ET and groundwater ET (ET_g) across phreatophyte areas are becoming more common. We build on previous studies and develop a transferable empirical relationship with uncertainty bounds between flux tower estimates of ET and a remotely sensed vegetation index, Enhanced Vegetation Index (EVI). Energy balance-corrected ET measured from 40 flux tower site-year combinations in the Great Basin was statistically correlated with EVI derived from Landsat imagery (r^2 = 0.97). Application of the relationship to estimate mean-annual ET_g from four HAs in western and eastern Nevada is highlighted and results are compared with previous estimates. Uncertainty bounds about the estimated mean ET_g allow investigators to evaluate if independent groundwater discharge estimates are “believable” and will ultimately assist local, state, and federal agencies to evaluate expert witness reports of ET_g, along with providing new first-order estimates of ET_g.

(KEY TERMS: evapotranspiration; basin water balance; phreatophyte; groundwater discharge; EVI; Landsat; remote sensing.)

Beamer, Jordan P., Justin L. Huntington, Charles G. Morton, and Greg M. Pohll, 2013. Estimating Annual Groundwater Evapotranspiration from Phreatophytes in the Great Basin Using Landsat and Flux Tower Measurements. *Journal of the American Water Resources Association* (JAWRA) 49(3): 518-533. DOI: 10.1111/jawr.12058

INTRODUCTION

Escalating concerns about current and future water supplies in the Great Basin have prompted numerous water budget studies focused on estimating groundwater recharge and discharge. Currently, many hydrologic studies in Nevada are focused on the appraisal of available water resources for inbasin use and interbasin transfers. As groundwater will

[1]Paper No. JAWRA-12-0108-P of the *Journal of the American Water Resources Association* (JAWRA). Received May 4, 2012; accepted November 19, 2012. **Discussions are open until six months from print publication.**

[2]Respectively, Formerly Graduate Student (Beamer), Graduate Program of Hydrologic Sciences, Desert Research Institute, University of Nevada - Reno, Reno, Nevada, Currently Graduate Student, School of Civil and Construction Engineering, 220 Owen Hall, Oregon State University, Corvallis, Oregon 97331; Assistant Research Professor (Huntington), Division of Hydrologic Sciences, Desert Research Institute, Reno, Nevada; Staff Remote Sensing & GIS Scientist (Morton), Division of Earth and Ecosystem Sciences, Desert Research Institute, Reno, Nevada; and Research Professor (Pohll), Division of Hydrologic Sciences, Desert Research Institute, Reno, Nevada (E-Mail/Beamer: jordan.beamer@gmail.com).

continue to be a water source for much of Nevada and the Great Basin, the need for accurate estimates of groundwater recharge and discharge is of utmost importance to water managers and decision makers.

Many drainage areas in the Great Basin are considered hydrologically closed, where the entire volume of groundwater recharge, derived from precipitation, is consumed by groundwater evapotranspiration (ET_g) along mountain front and valley floor areas. Estimating the natural groundwater recharge from precipitation in a given hydrographic area (HA) is very difficult and often has significant uncertainty, therefore it is often quantified by estimating the natural groundwater discharge (Maxey and Eakin, 1949; Nichols, 2000). Thus, groundwater discharge estimates provide constraints on recharge and/or interbasin flow estimates, acting as control points for HA or larger flow system water budgets. Prior estimation of ET_g, its spatial and temporal variability, and the uncertainty of the estimates are critical in the successful calibration of basin-scale groundwater models (Senay *et al.*, 2011). The perennial yield of a HA is typically based on the estimated steady-state recharge and/or natural groundwater discharge. The natural discharge is effectively the limit as to the maximum amount of groundwater that can be captured under the perennial yield concept.

Evapotranspiration is the rate at which water is transferred from land and plant surfaces to the atmosphere. ET is a function of the at-surface radiative and advective energy, and varies in time and space depending on vegetation type and density, soil type and moisture, and local-to-regional meteorological factors such as humidity and precipitation. In HAs with deep groundwater and limited surface water resources, water loss through ET will be limited to local precipitation amount. However, in basins with a shallow groundwater, ET rates often exceed precipitation rates, where facultative and obligate phreatophytes are able to access the groundwater (Devitt *et al.*, 2011).

Because most valley floor areas in the Great Basin are fairly large in size, uncertainty in the estimated ET_g rate from phreatophyte areas leads to a large uncertainty in the overall water budget, especially the groundwater budget (Nichols, 1993). Many recent studies have assessed ET_g rates of phreatophyte communities in the Great Basin using micrometeorological, energy balance, and remote sensing techniques (Laczniak *et al.*, 1999; Reiner *et al.*, 2002; Harrington *et al.*, 2004; Maurer *et al.*, 2005; Steinwand *et al.*, 2006; Groeneveld *et al.*, 2007; Moreo *et al.*, 2007; DeMeo *et al.*, 2008; Allander *et al.*, 2009; Devitt *et al.*, 2011; Huntington *et al.*, 2011). Relating flux tower estimates of ET to space-borne remote sensing data (e.g., Landsat, MODIS) allows for spatial scaling of ET to the entire HA. These studies have produced and analyzed multiyear, high-quality climatic and surface energy balance (SEB) datasets for various phreatophyte species and climates across the Great Basin, which has created the unique opportunity to compile, analyze, and develop a transferable, data-driven approach to estimate phreatophyte ET using remote sensing.

There are two general remote sensing approaches for estimating spatial distributions of ET, a SEB and vegetation index (VI) approach. Remotely sensed SEB methods use surface reflectance and surface temperature data to formulate a solution of the surface energy budget (Kalma *et al.*, 2008). One SEB approach estimates net radiation (R_n), soil heat flux (G), and sensible heat flux (H) and then calculates the latent heat flux (LE) as a residual. All terms are usually expressed in W/m^2. The LE residual approach is expressed as

$$\mathrm{LE} = R_n - G - H \tag{1}$$

where ET is LE/λ (expressed in $kg/m^2/s$), and λ is the latent heat of vaporization (J/kg). In arid landscapes with hot, dry conditions and sparse vegetation, application of the SEB approach can be difficult because values of $R_n - G$ and H are typically large. This can lead to potential error in LE that will exceed the LE rate itself. This situation becomes even more of a problem when estimates of ET_g are made. Annual ET_g is estimated as

$$\mathrm{ET_g} = \mathrm{ET_a} - \mathrm{PPT} \tag{2}$$

where ET_g is the annual groundwater component of ET, ET_a is the annual actual ET, and PPT is the annual precipitation. In addition, because Landsat satellites have 16-day return intervals, ET derived from local precipitation events that occur between image acquisitions is often not detected. This “missing” ET derived from precipitation can have a significant impact on the estimated annual ET_g.

Relating annual flux tower ET estimates to remotely sensed VIs is advantageous because it allows point estimates of annual ET to be spatially distributed to the total discharge area using seasonally averaged or peak annual VI values as a scalar. These relationships can be used across large areas with multiple sensor systems, such as Landsat or MODIS satellites. Nichols (2000) empirically related ET_g to plant cover for phreatophyte areas in the southern and central Great Basin by relating the Modified Soil Adjusted Vegetation Index (MSAVI) to plant cover and ultimately ET_g. However, estimating ET_g as a function of plant cover alone does not take into account regional and local variability in precipitation and atmospheric water demand. Devitt *et al.,* (2011) recently relied on Eddy covariance (EC) estimates of ET_a from phreatophyte areas in three HAs located in eastern Nevada to develop empirical relationships between ET_a and the Normalized Difference Vegetation Index (NDVI) computed from Landsat data. Devitt *et al.,* (2011) found that precipitation and reference ET (ET_o) had significant influence on the estimated ET_a. As such, empirical relationships developed from estimates of ET_a and VIs alone are largely HA specific, meaning that they are nontransferable between HAs due to differences in precipitation and ET_o. For example, two HAs may share similar vegetation greenness, but have vastly different annual ET_a and ET_g due to differences in climate. In addition, having a relatively small number of ET_a observations to develop empirical relationships results in low statistical strength and increases the uncertainty of prediction.

OBJECTIVES

The objectives of this study are threefold: (1) compile and utilize a combined total of 40 years of micrometeorological data collected by 26 Bowen Ratio (BR) and EC systems located primarily in phreatophyte vegetation in Nevada, (2) develop a robust empirical relationship with uncertainty bounds between annual ET_a and a selected satellite-derived VI that takes into account local and regional precipitation and atmospheric water demands so that the relationship can be transferred across multiple HAs, and (3) apply the developed empirical functions in HAs of interest and compare the predicted ET_g and associated uncertainty to previously estimated ET_g volumes.

STUDY SITES AND METEOROLOGICAL DATA

Study sites are located in western, eastern, and southern Nevada, within the Great Salt Lake, Death Valley, Colorado River, Walker River, and Carson River regional flow systems (Figure 1). The regional climate across the study sites is arid to semiarid, where the mean-annual precipitation ranges from 150 to 250 mm/yr with approximately 40-80% of the precipitation occurring during the winter months. Mean monthly temperature varies across the study sites where the mean monthly maximum temperature ranges from 30 to 40°C in July, and the mean monthly minimum temperature ranges from −2 to −10°C in January. Vegetation surrounding the study sites primarily consists of fairly homogeneous and extensive phreatophyte shrub species of greasewood (*Sarcobatus vermiculatus*), rabbitbrush (*Chrysothamnus nauseosus*), salt grass (*Distichlis spicata*), sagebrush (*Artemisia tridentata*), arrowweed (*Pluchea sericea*), salt cedar (*Tamarix ramosa*), mesquite (*Prosopis spp.*), and wolfberry (*Lycium pallidum*). Five of the sites were surrounded by subirrigated pasture grasses and flood irrigated alfalfa managed for water fowl habitat. Depth to groundwater at the study sites ranged from 0 to 10 m below land surface. Micrometeorological stations at the study sites consisted of EC and/or BR towers operated and maintained by the U.S. Geological Survey (USGS) and Desert Research Institute (DRI) (Reiner *et al.*, 2002; Maurer *et al.,* 2005; Moreo *et al.*, 2007; DeMeo *et al.*, 2008; Allander *et al.*, 2009; Arnone *et al.*, 2009). Station data were chosen based on the quality and criteria that each site had at least one full year of ET_a, PPT, and meteorological data to compute ET_o. Daily average meteorological measurements of solar radiation, air temperature, vapor pressure, and wind speed were used to compute ET_o. Daily PPT totals for each site-year were collected either at a rain gauge located at the tower site or from a nearby station. Specifics regarding data processing and micrometeorological instrumentation at the study sites can be found in source publications (Reiner *et al.*, 2002; Maurer *et al.,* 2005; Moreo *et al.*, 2007; DeMeo *et al.*, 2008; Allander *et al.*, 2009; Arnone *et al.*, 2009) and Beamer (2011). Study site locations, altitude, period of record used, vegetation type, and study sources are shown in Table 1.

APPROACH

Normalization procedures are attractive because they allow formulae to be expressed in a dimensionless form which is normalized by maximum or minimum values, where these extreme values can change depending on location or environment (Kahler and Brutsaert, 2006). To account for spatial variability in climate, we use annual PPT and ET_o to normalize ET_a similar to the approach outlined by Groeneveld *et al.* (2007). Normalized ET_a is calculated as

$$ET^* = (ET_a - PPT)/(ET_o - PPT) \tag{3}$$

where ET* is normalized ET_a (dimensionless), PPT is total water year precipitation, and ET_o is total water year ET_o. Groeneveld *et al.* (2007) showed that NDVI was a competent estimator of ET_a for three separate studies conducted in arid and semiarid phreatophyte

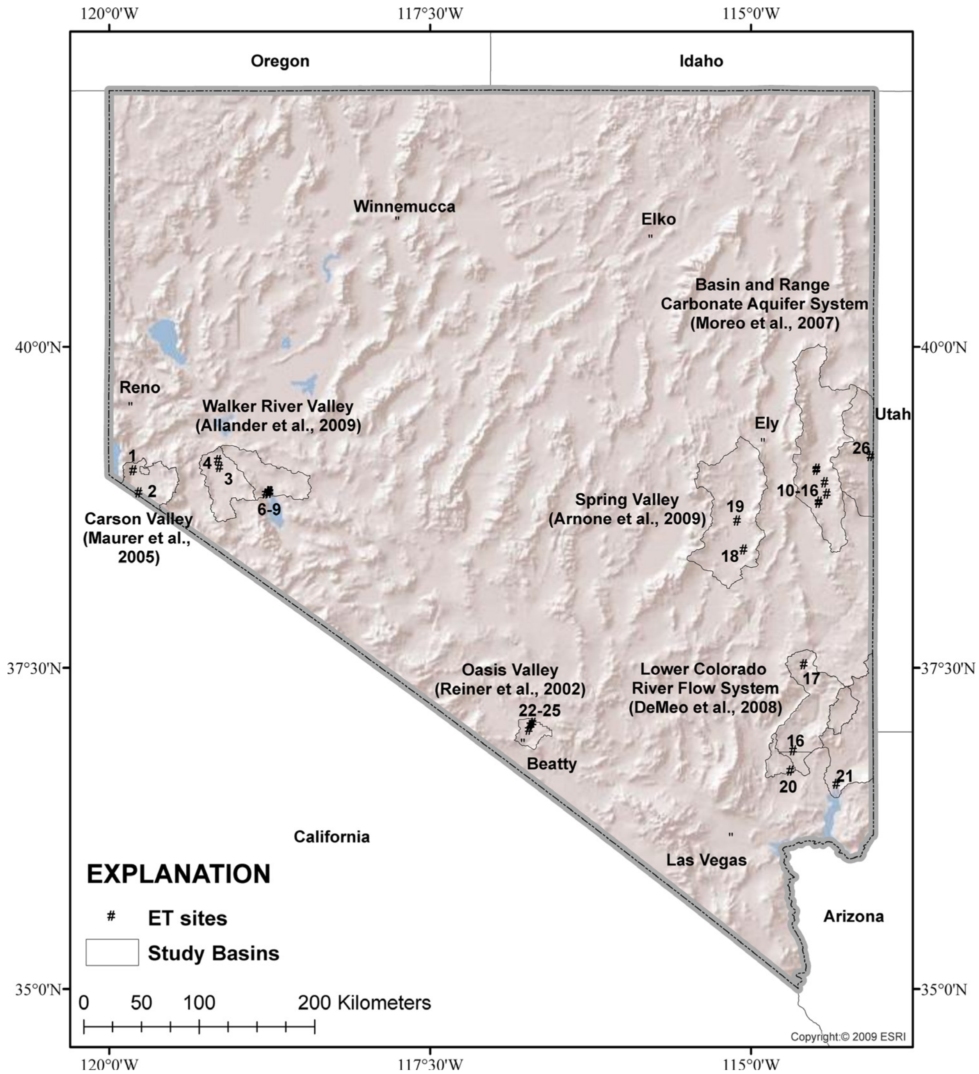

FIGURE 1. Map Showing the Study Area Extents for the Six Evapotranspiration (ET) Studies (Reiner *et al.*, 2002; Maurer *et al.*, 2005; Moreo *et al.*, 2007; Arnone *et al.*, 2009; DeMeo *et al.*, 2008; Allander *et al.*, 2009) as well as the Location of the ET Sites. Numbers refer to list in Table 1.

areas in California, New Mexico, and Colorado. While ET station source area NDVI values from a single midsummer Landsat scene related well with ET_a ($r^2 = 0.94$), the relationship was improved by subtracting PPT and normalizing by the ET_o minus PPT to form ET* ($r^2 = 0.96$). By using a normalization procedure to compute ET* for 40 site-years, we build on previous works relating VIs to ET_a and ultimately allow for robust application to estimate ET_a and ET_g across variable climates within the Great Basin.

Micrometeorological and Meteorological Data Preparation

Micrometeorological and meteorological data at 20-30-minute time steps were acquired from the USGS and DRI for all 26 sites. These data were derived from a mix of EC and BR flux towers. The primary advantage of the EC approach is that it estimates LE and H independent of the available energy ($R_n - G$), making it more advantageous over the BR approach in which available energy is used to calculate LE, effectively forcing energy balance closure (EBC). In fact, independent measurements of LE and H frequently result in closure error where the measured quantities $R_n - G$ do not equate to LE + H. Meyers and Baldocchi (2005) suggested that the mean uncertainty for ET measurement from a perfectly designed and maintained EC system can be as good as 10%. Foken (2008) suggests that inadequate measurement of longwave eddies is a main reason why turbulent fluxes (H and LE) are typically undermeasured with EC systems. To utilize surface flux data and validate or develop land surface models requires that the conservation of energy be satisfied; therefore it is sug-

TABLE 1. General Information from Evapotranspiration (ET) Stations Used in This Research (locations shown in Figure 1).

Site	Site ID	Vegetation Type	Lat., °N	Long., °W	Altitude, m	Period of Data Collection	Study Source
1	ET-1	Greasewood/rabbitbrush	39.029	−119.807	1,421	10/03-09/04	2
2	ET-8	Irrigated pasture grass	38.859	−119.763	1,471	10/03-09/04	2
3	B-01	Nonirrigated alfalfa	39.055	−119.134	1,326	04/05-03/07	6
4	B-11	Irrigated alfalfa	39.108	−119.146	1,317	03/05-02/07	6
5	GRE	Greasewood	38.854	−118.743	1,224	03/05-02/06	6
6	GRE-2	Greasewood	38.854	−118.743	1,224	10/06-09/07	6
7	SAL	Salt grass	38.865	−118.742	1,222	03/05-02/06	6
8	SAL-2	Salt grass	38.867	−118.752	1,224	10/06-09/07	6
9	TAM	Salt cedar	38.851	−118.773	1,223	04/05-03/07	6
10	SPV-1	Greasewood/rabbitbrush	38.778	−114.468	1,764	09/05-08/07	3
11	SPV-2	Greasewood/rabbitbrush	38.786	−114.466	1,762	09/05-08/07	3
12	SPV-3	Mixed grasses	38.937	−114.421	1,764	09/05-08/07	3
13	SV-4	Mixed grasses	38.848	−114.404	1,773	04/07-11/09	4
14	SV-5	Greasewood/rabbitbrush	39.032	−114.485	1,760	04/07-06/10	4
15	SV-6	Greasewood/rabbitbrush	39.043	−114.483	1,756	04/07-06/10	4
16	LMVW	Arrowweed	36.850	−114.666	579	02/03-09/06	5
17	UMVW	Rabbitbrush	37.520	−114.583	1,250	02/03-09/06	5
18	WRV-1	Greasewood	38.414	−115.051	1,601	09/05-08/07	3
19	WRV-2	Greasewood	38.640	−115.102	1,622	09/05-08/07	3
20	MR	Mesquite	36.691	−114.688	503	02/03-09/06	5
21	VR	Salt cedar	36.588	−114.328	370	02/03-09/06	5
22	MOVAL	Wire grass/salt grass	37.011	−116.723	1,125	01/98-01/00	1
23	UOVLO	Greasewood	37.045	−116.708	1,177	08/98-08/00	1
24	UOVMD	Salt grass	37.047	−116.711	1,176	08/98-08/00	1
25	UOVUP	Wolfberry/rabbitbrush	37.064	−116.694	1,198	08/98-08/00	1
26	SNV-1	Greasewood	39.140	−114.062	1,558	09/05-08/07	3

Note: Numbers in study source column indicate particular study: (1) Reiner *et al.* (2002); (2) Maurer *et al.* (2005); (3) Moreo *et al.* (2007); (4) Arnone *et al.* (2009); (5) DeMeo *et al.* (2008); and (6) Allander *et al.* (2009).

gested that the measured energy budget be closed by some accepted approach (Twine *et al.*, 2000; Foken, 2008). In addition, because we rely on both EC and BR systems to develop a combined database of ET_a, it is appropriate that EBC corrections to the EC data be made so that EC and BR datasets are comparable. There are various strategies to apply EBC corrections. If the source of the error is thought to be from the hygrometer, EBC can be achieved by assuming all of the error resides in LE. More commonly the error is assumed to be due to loss of covariance that affects both H and LE in similar proportions. This EBC correction method assumes that the Bowen ratio β (H/LE) (Bowen, 1926) is measured correctly, and thus adjusts the magnitude of LE and H so that EBC can be achieved. Ultimately, because LE fluxes from EC towers are being directly compared with those from BR systems, EBC correction of the measured LE while maintaining the measured β is a reasonable approach.

EC-derived energy balance data were evaluated by calculating the energy budget ratio (EBR) as

$$\mathrm{EBR} = (R_\mathrm{n} - G)/(\mathrm{LE} + H). \quad (4)$$

Computed EBR over 22 site-years of EC data indicates that none of the sites achieved complete EBC. EBC corrections to LE and/or H were performed following the Bowen ratio procedure outlined by Lee (1998), Blanken *et al.* (1997), and Twine *et al.* (2000), which adjusts LE and H for 30-minute time steps when R_n is positive (day time) to force the EBR to unity, while maintaining a constant Bowen ratio (β). Corrected LE and H were calculated as

$$\mathrm{LE_{corr}} = (R_\mathrm{n} - G)/(1 + \beta) \quad (5)$$

and

$$H_\mathrm{corr} = \mathrm{LE_{corr}} \times \beta. \quad (6)$$

A potential limitation of this approach is the assumption that $R_\mathrm{n} - G$ is correctly measured, however, R_n tends to be underestimated rather than overestimated, and G is typically slightly underestimated due to inadequate estimation of heat storage, likely resulting in a similar available energy term (Halldin and Lindroth, 1992; Liebethal and Folken, 2007; Foken, 2008). The Bowen ratio EBC approach has been extensively applied and is suggested as the most reasonable approach when suspected errors in individual energy balance components such as $R_\mathrm{n} - G$ are not known and a first-order estimate of the EBC corrections is required (Blanken *et al.*, 1997; Lee, 1998; Twine *et al.*, 2000; Foken, 2008). Following cor-

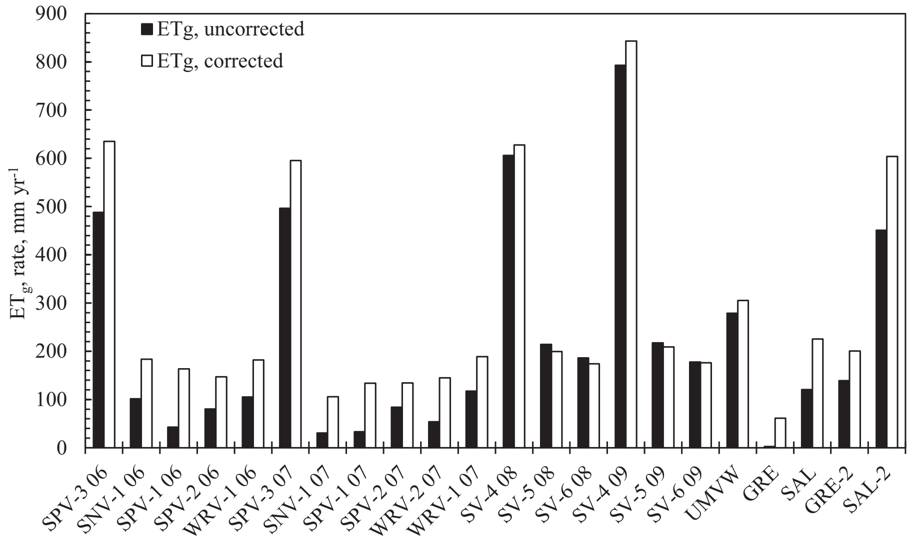

FIGURE 2. Comparison of Annual Groundwater Evapotranspiration (ET_g) Rates from 22 Site-Years of Eddy Covariance Data with Uncorrected (raw) and Corrected (via β variant approach).

rection of the daytime LE for 22 EC sites, ET_a estimates increased by an average of 22% (65 mm/yr). Following removal of PPT, an adjusted value of annual ET_g was calculated at the EC sites (Figure 2).

ET data from all BR and EC sites were summed to daily totals, and these totals were used to compute annual water year ET_a. Quality assurance and quality control procedures outlined in Allen *et al.* (2011) were used to screen meteorological data of solar radiation, humidity, temperature, and wind speed. Daily meteorological data of solar radiation, humidity, temperature, and wind speed were used to compute the ET_o following the American Society of Civil Engineers (ASCE) Standardized Penman-Montieth (PM) equation for a grass reference surface (Allen *et al.*, 2005). ET_o was calculated at each site over the same time period that ET_a and PPT were computed such that ET* would be consistent with respect to the period of record of each input variable. In a plot comparing water year ET_a and ET_o for all 40 site-years of data, sites with high ET_a had noticeably less ET_o than sites with low ET_a (Figure 3).

Landsat 5 TM Satellite Data Preparation

Landsat 5 TM satellite data acquired during ET measurement periods were used to empirically relate three remotely sensed VIs with ET* derived at flux tower locations. Landsat 5 TM radiometer measures visible, reflected, and thermal infrared radiation in seven wavelength bands ranging from 0.45 to 12.5 μm. Reflectance data from these bands were used to calculate different VIs once radiometric and atmospheric corrections were completed following Allen *et al.* (2007) and Tasumi *et al.* (2008). The scene processing steps included: (1) perform radiometric and atmospheric corrections for each midsummer Landsat TM image chosen; (2) calculate VIs of Enhanced Vegetation Index (EVI) (Nagler *et al.*, 2005), MSAVI (Qi *et al.*, 1994), and NDVI; (3) extract the mean source area VI values around each flux tower for each image; and (4) pair source area VI and annual ET* values for each flux tower site for multiple years. NDVI, EVI, and MSAVI images were created from each Landsat TM image using the following equations

$$\mathrm{NDVI} = (\rho_{\mathrm{NIR}} - \rho_{\mathrm{Red}})/(\rho_{\mathrm{NIR}} + \rho_{\mathrm{Red}}) \quad (7)$$

$$\mathrm{EVI} = 2.5(\rho_{\mathrm{NIR}} - \rho_{\mathrm{Red}})/(\rho_{\mathrm{NIR}} + 6\rho_{\mathrm{Red}} + 7.5\rho_{\mathrm{Blue}} + 1) \quad (8)$$

$$\mathrm{MSAVI} = (\rho_{\mathrm{NIR}} - \rho_{\mathrm{Red}})(1 + L)/(\rho_{\mathrm{NIR}} + \rho_{\mathrm{Red}} + L) \quad (9)$$

$$L = 1 - (2s(\rho_{\mathrm{NIR}} - \rho_{\mathrm{Red}})(\rho_{\mathrm{NIR}} - s\rho_{\mathrm{Red}}))/(\rho_{\mathrm{NIR}} + \rho_{\mathrm{Red}}) \quad (10)$$

where ρ is the at-surface reflectance, NIR is near infrared waveband from 0.76 to 0.90 μm, Red is waveband from 0.63 to 0.69 μm, Blue is waveband from 0.45 to 0.52 μm, s is the slope of the soil line assumed to equal 1.06, and L is a soil adjustment factor (Qi *et al.*, 1994). NDVI, MSAVI, and EVI values were spatially averaged for 100-m footprints around all 26 ET flux tower locations using individual midsummer TM scenes shown in Table 2. Previous

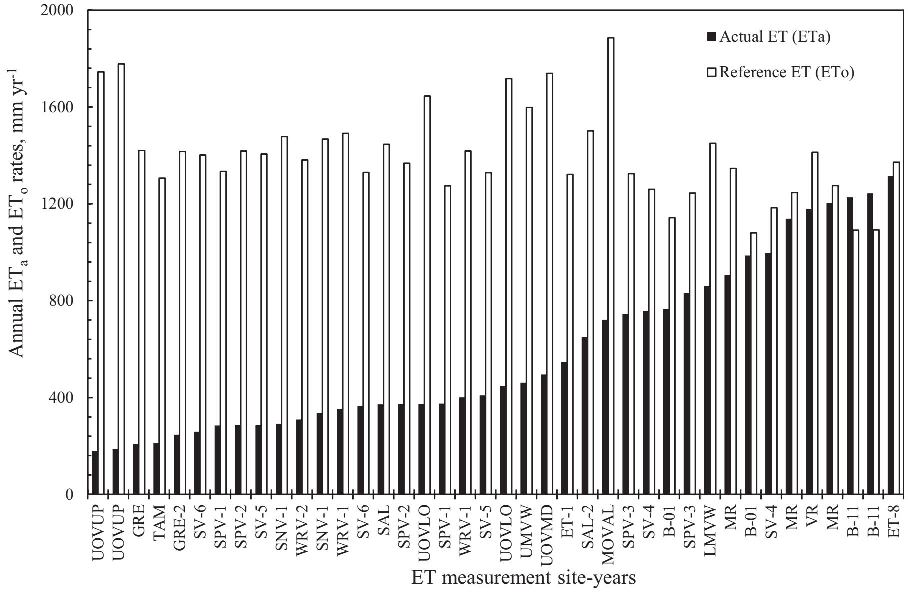

FIGURE 3. Comparison of Annual Actual Evapotranspiration (ET_a) and Reference ET (ET_o) Rates for 40 Site-Years Used in Study. As ET_a rates increase to the maximum value, ET_o generally declines and approaches ET_a value.

studies suggest that the time period from June to August is the most representative period to characterize peak health and vigor of phreatophyte vegetation in the Great Basin (Groeneveld *et al.*, 2007; Smith *et al.*, 2007; Allander *et al.*, 2009). A sensitivity analysis of average VIs over footprint radius size of 100, 200, and 300 m showed negligible differences for shrubland sites, but for riparian sites the impacts of nonriparian areas increased with larger footprint radius. To avoid contaminating VI signals in riparian areas, and given that an estimated 80% of the turbulent fluxes measured at many stations used in this work originates within a 100 m radius of the flux site (Moreo *et al.*, 2007; Allander *et al.*, 2009), we chose to use a 100-m radius footprint for VI spatial averaging.

VI and ET Regression Analysis

Second-order polynomial regression analysis was performed using ET_a and ET* from the flux towers as the dependent variable and each of the three respective mean VI values as the independent variable. Following testing of the three VIs as predictors of ET, EVI was chosen based on having the lower sum of squared error and highest r^2 of 0.96 (Table 3). Other regression models were also tested; however, the second-order polynomial model provided the best fit (Figure 4). In addition, the shape of the regression is consistent with complementary feedbacks that exist between ET_a and ET_o in phreatophyte shrub environments (Huntington *et al.*, 2011), where ET* asymptotically approaches the maximum ET* as EVI increases with increased surface moisture. The second-order polynomial model equation for both ET_a and ET* formulation is

$$ET = \beta_0 + \beta_1 EVI + \beta_2 EVI^2, \qquad (11)$$

where ET is the ET_a or ET*, EVI is mean source area Enhanced Vegetation Index, and β_0, β_1, β_2 are the regression coefficients which for ET* are −0.196, 2.904, and −1.592 (Table 4). Equation (11) takes the same form for both ET_a-EVI and ET*-EVI regression analysis, but will be used to describe ET* calculation for the remainder of the study. Upper and lower 90% confidence and prediction intervals were also formulated for ET*, with prediction bands shown in Figure 5. The confidence interval represents the degree of confidence in the mean, and is computed when the center of mass of the data is the statistic of interest. The prediction interval indicates the degree of confidence in where you can expect to see the next data point sampled (e.g., degree of confidence for an EVI and ET* pair to fall with the specified significance level of 10% in this case). The prediction intervals in Figure 5 are wider than confidence intervals because they take into account variability in single data points along with estimating the center of the distribution (Helsel and Hirsch, 2002).

Estimating ET_a and ET_g

Once EVI values are used to estimate ET*, ET_a is estimated similar to Groeneveld *et al.* (2007) as

$$ET_a(\text{estimated}) = (ET_o - PPT)ET^* + PPT \quad (12)$$

By subtracting the annual PPT, the groundwater component of ET, ET_g is estimated as

TABLE 2. Date of Acquisition, Path/Row, and TM Sensor of Landsat Scenes Selected for VI-ET Analysis.

Study Area	Date	Sensor	Path	Row
BARCAS	7/15/2006	TM5	39	33
BARCAS	5/31/2007	TM5	39	33
Spring Valley	6/20/2008	TM5	39	33
Spring Valley	7/7/2009	TM5	39	33
Carson Valley	7/7/2004	TM5	43	33
Colorado River flow system	6/25/2004	TM5	39	34/35
Colorado River flow system	6/26/2005	TM5	39	34/35
Colorado River flow system	6/29/2006	TM5	39	34/35
Oasis Valley	6/30/1998	TM5	40	34
Oasis Valley	6/17/1999	TM5	40	34
Oasis Valley	6/21/2000	TM5	40	34
Walker River Valley	6/15/2005	TM5	42	33
Walker River Valley	6/18/2006	TM5	42	33
Walker River Valley	6/21/2007	TM5	42	33

Note: BARCAS, Basin and Range Carbonate Aquifer Study.

TABLE 3. Comparison of Relationship of Annual ET with Enhanced Vegetation Index (EVI), Modified Soil Adjusted Vegetation Index (MSAVI), and Normalized Difference Vegetation Index (NDVI).

Vegetation Index	Equation of Best Fit	r^2
EVI	$ET = -96.6 \times EVI^2 + 139.7 \times EVI - 2.56$	0.96
MSAVI	$ET = -125.2 \times MSAVI^2 + 157.8 \times MSAVI - 1.7$	0.95
NDVI	$ET = -41.7 \times NDVI^2 + 94.5 \times NDVI - 0.24$	0.92

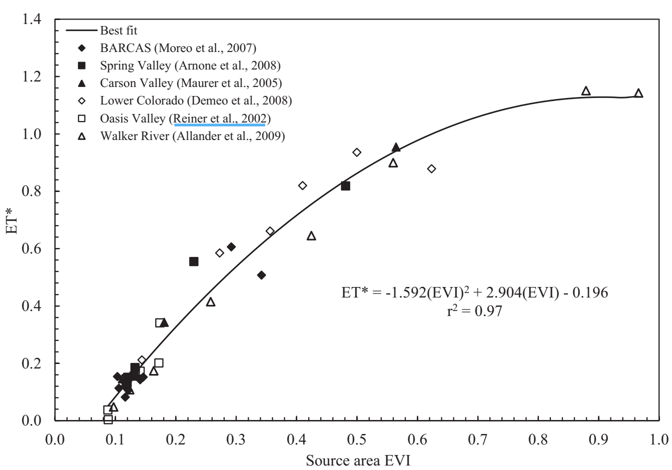

FIGURE 4. Peak Enhanced Vegetation Index (EVI)-ET* Data Pairs for the 40 Site-Years of Nevada Bowen Ratio and Eddy Covariance Stations Analyzed in This Study. Symbols represent the six different ET studies. Best-fit curve, predictive equation, and r^2 value provided.

TABLE 4. β-Coefficients for the Model Equation, 90% Confidence Interval (CI), and 90% Prediction Interval (PI), and x-Intercept for the Quadratic Equation Relating EVI and ET*.

Equation	β_0	β_1	β_2	Root (x-int.)
Polynomial curve (model)	−0.196	2.904	−1.592	0.068
Upper 90% CI band	−0.177	2.891	−1.528	0.063
Lower 90% CI band	−0.214	2.918	−1.655	0.077
Upper 90% PI band	−0.104	2.889	−1.557	0.037
Lower 90% PI band	−0.287	2.919	−1.626	0.104

$$ET_g(\text{estimated}) = (ET_o - PPT)ET^* \quad (13)$$

From Equation (13) EVI can be transformed into ET_g so that the annual ET_g volume can be estimated from a given phreatophyte groundwater discharge area. This approach was validated by using source area EVI to calculate ET* for all 40 site-years of *in situ* data, then ET_o and PPT were used to estimate ET_g. The residual error of ET_g (estimated-observed) is well balanced indicating the algorithm can model ET_g accurately for a wide range of vegetation and climate conditions (Figure 6). Errors tend to be small and positive at ET_g values less than 400 mm/yr, unbiased but large between 400 and 800 mm/yr, small and negative greater than 800 mm/yr. Positive error indicates that ET* is overestimated because of a high source area EVI value, whereas negative error indicates underestimation of ET* because of a low EVI value. Table 5 lists ET_a, ET_o, PPT, ET_g, ET*, estimated ET*, estimated ET_g, and estimated residuals for each site.

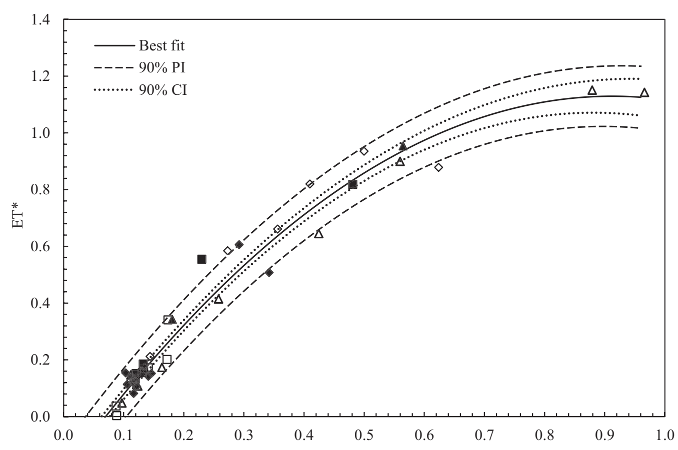

FIGURE 5. EVI- ET* Data with Best-fit Curve, Upper/Lower 90% Confidence and Prediction Interval Bands.

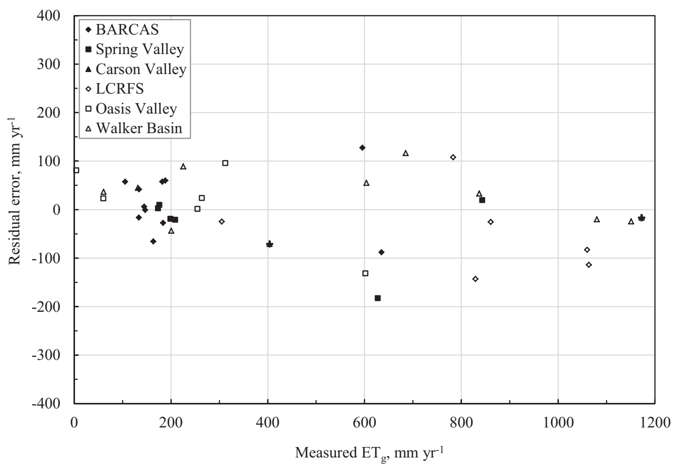

FIGURE 6. Residual Error of Annual Groundwater Evapotranspiration (ET_g) Predicted from Equation (13) Using EVI, Annual Reference ET, and Annual Precipitation *vs.* Measured ET_g Values.

Application for Estimating ET_g in Western and Eastern Nevada

Equations (11) and (13) were applied to phreatophyte discharge areas in four different HAs in western and eastern Nevada. The four HAs of Dry Valley, Red Rock Valley, White River Valley, and Spring Valley were selected based on the numerous studies that have been conducted and datasets generated. Previous studies have delineated phreatophyte areas using field mapping and remote sensing techniques, collected meteorological data (ET_o and PPT), and have provided independent estimates of the annual ET_g (Rush and Glancy, 1967; Nichols, 2000; Berger *et al.*, 2004; Welch *et al.*, 2007). This allowed for a unique opportunity to perform an independent comparison with previous work. White River Valley and Spring Valley have areas of 4,140 km^2 (1,023,000 acres) and 4,318 km^2 (1,067,000 acres), respectively, whereas Dry Valley and Red Rock Valley are much smaller in size at 212 km^2 (52,500 acres) and 109 km^2 (27,000 acres), respectively.

Steps taken for estimating the ET_g volume for the four HAs included: (1) selecting a representative mean-annual water year based on historical annual PPT records from a valley floor weather station within the HA, (2) selecting single midsummer Landsat scenes for respective HAs and mean-annual water years, processing the scenes to at-surface reflectance, and computing EVI, (3) delineating the phreatophyte area within each HA using data from previous investigations, (4) estimating ET* for each pixel within the phreatophyte area using mean, and upper and lower confidence and prediction interval regression equations, and (5) estimating the annual ET_g by applying respective annual ET_o and PPT measured within or near the phreatophyte areas.

After analyzing PPT records for COOP and RAWS weather stations in respective HAs, water year 2006 was determined to have annual PPT amounts near the average annual amount for each station. Single midsummer Landsat TM scenes were selected covering each HA and phreatophyte area of interest and are listed in Table 6. Simple criteria for scene selection were as follows: (1) the scenes are completely clear of cloud/smoke within the delineated phreatophyte boundary, (2) there has been no major precipitation event in the two weeks leading up to scene acquisition, and (3) the vegetation signal from the phreatophyte areas is easily distinguished (greener, high EVI) from the surrounding nonphreatophyte areas, indicating plants are utilizing shallow groundwater stores. EVI was calculated using the computed at-surface reflectance, and pixel values were extracted from within the delineated phreatophyte boundary for each HA.

Groundwater discharge estimates for the HAs in this work are intended to represent those of predevelopment conditions, which was also assumed in previous work for these HAs. As such, following an approach described in Welch *et al.* (2007) and Welborn and Moreo (2007), EVI values for areas identified as irrigated cropland were replaced with EVI values that equal the area-weighted average EVI value occurring in the groundwater discharge area, representative of mixed phreatophyte vegetation.

Estimates of PPT and ET_o for water year 2006 were derived from rain gauge and meteorological data collected from within phreatophyte areas for each respective HA, or in an adjacent phreatophyte area located nearby with similar meteorologic and hydrologic conditions (Table 6). Equations (11-13) were used to formulate estimates of ET*, ET_a, and ET_g for each pixel within the phreatophyte boundary, and total volumes of ET_a and ET_g were subsequently computed for phreatophyte areas within each HA.

RESULTS

Mean-Annual Phreatophyte ET Estimates

Using surface reflectance data from a single midsummer Landsat 5 scene along with ET_o and PPT data measured within representative phreatophyte areas, a first-order estimate of phreatophyte ET was calculated for four HAs in western and eastern Nevada. Mean ET_g rates, total ET_g volumes, mean ET_g rate prediction intervals, and total ET_g volume prediction intervals for the phreatophyte areas of all

TABLE 5. Summary of Measured ET Data for All 40 Site-Years Along with Predicted ET* and Groundwater Evapotranspiration (ET_g).

Site	Year	EVI	ET_a (mm/yr)	ET_o (mm/yr)	PPT (mm/yr)	ET_g (mm/yr)	ET*	Est. ET*	Est. ET_g (mm/yr)	Residual (mm/yr)
BARCAS study (Moreo *et al.*, 2007)										
SPV-3	2006	0.2922	832	1,244	197	634.9	0.606	0.5221	547.1	−87.8
SNV-1	2006	0.1138	337	1,468	153	183.7	0.139	0.1190	156.4	−27.3
SPV-1	2006	0.1034	375	1,274	212	163.6	0.154	0.0924	98.2	−65.4
SPV-2	2006	0.1173	373	1,368	226	146.9	0.129	0.1280	146.2	−0.7
WRV-1	2006	0.1462	401	1,418	219	182.1	0.152	0.1998	239.5	57.4
SPV-3	2007	0.3420	746	1,324	151	595.5	0.507	0.6163	723.2	127.7
SNV-1	2007	0.1166	291	1,478	186	105.5	0.082	0.1262	163.0	57.5
SPV-1	2007	0.1060	285	1,334	151	133.8	0.113	0.0991	117.3	−16.6
SPV-2	2007	0.1217	285	1,418	151	134.4	0.106	0.1391	176.3	41.9
WRV-2	2007	0.1158	309	1,382	164	145.0	0.119	0.1240	150.9	6.0
WRV-1	2007	0.1412	353	1,491	164	188.7	0.142	0.1874	248.7	59.9
Average						237.6	0.2	0.2	251.5	13.9
Spring Valley (Arnone *et al.*, 2009)										
SV-4	2008	0.2300	756	1,260	129	627.6	0.555	0.3931	445.0	−182.7
SV-5	2008	0.1207	286	1,406	87	199.2	0.151	0.1365	180.0	−19.2
SV-6	2008	0.1197	259	1,402	85	173.8	0.132	0.1339	176.3	2.5
SV-4	2009	0.4812	997	1,184	154	843.2	0.819	0.8376	862.7	19.5
SV-5	2009	0.1327	409	1,329	200	209.2	0.185	0.1665	188.1	−21.1
SV-6	2009	0.1312	366	1,330	189	176.3	0.155	0.1629	185.7	9.4
Average						371.6	0.3	0.3	339.6	−31.9
Carson Valley (Maurer *et al.*, 2005)										
ET-1	2004	0.1810	547	1,322	143	404.0	0.343	0.2828	333.4	−70.6
ET-8	2004	0.5650	1,315	1,372	143	1,172.3	0.954	0.9407	1,156.1	−16.2
Average						788.2	0.6	0.6	744.7	−43.4
Lower Colorado flow system (DeMeo *et al.*, 2008)										
MR	2004	0.5000	1,203	1,276	143	1,059.9	0.936	0.8627	977.3	−82.5
VR	2004	0.4100	1,179	1,413	116	1,063.4	0.820	0.7321	949.6	−113.7
MR	2005	0.6238	1,139	1,247	356	782.9	0.878	0.9997	891.1	108.2
MR	2006	0.3563	905	1,346	44	860.7	0.661	0.6418	835.4	−25.3
LMVW	2006	0.2729	860	1,450	31	829.0	0.584	0.4834	685.9	−143.1
UMVW	2006	0.1440	461	1,598	156	305.2	0.212	0.1944	280.3	−24.8
Average						816.9	0.7	0.7	770.0	−46.9
Oasis Valley (Reiner *et al.*, 2002)										
MOVAL	1999	0.1740	721	1,886	119	602.1	0.341	0.2663	470.5	−131.6
UOVLO	1999	0.1333	374	1,645	119	255.2	0.167	0.1681	256.5	1.4
UOVUP	1999	0.0876	180	1,745	119	60.5	0.037	0.0513	83.3	22.8
UOVLO	2000	0.1412	447	1,717	182	264.3	0.172	0.1876	288.0	23.7
UOVUP	2000	0.0885	187	1,778	182	4.7	0.003	0.0535	85.4	80.7
UOVMD	2000	0.1722	495	1,739	182	312.6	0.201	0.2623	408.3	95.7
Average						249.9	0.2	0.2	265.3	15.4
Lower Walker River Valley (Allander *et al.*, 2009)										
GRE	2005	0.0973	208	1,421	147	61.2	0.048	0.0767	97.7	36.6
SAL	2005	0.1638	372	1,446	147	225.5	0.174	0.2422	314.6	89.1
GRE-2	2007	0.1121	246	1,416	46	200.7	0.147	0.1147	157.2	−43.5
SAL-2	2007	0.2580	649	1,502	46	603.8	0.415	0.4526	659.1	55.3
B-11	2005	0.9664	1,227	1,092	147	1,080.1	1.143	1.1226	1,060.9	−19.2
B-01	2005	0.5600	987	1,080	150	837.0	0.899	0.9352	870.3	33.3
B-11	2006	0.8794	1,244	1,093	93	1,150.9	1.151	1.1271	1,127.2	−23.7
B-01	2006	0.4247	766	1,143	81	684.9	0.645	0.7552	801.8	116.8
TAM	2006	0.1237	213	1,306	81	131.8	0.108	0.1441	176.5	44.8
Average						552.9	0.5	0.6	585.0	32.2

four HAs are shown in Table 6. Mean ET_g rates were calculated as the area-weighted average of the pixel ET_g rate for the phreatophyte area. Total ET_g volumes were calculated as a sum of the pixel ET_g volumes. Maps of ET_g within delineated phreatophyte boundaries show the spatial variation in phreatophyte ET, where the highest rates are concentrated around areas known to have shallow groundwater or are impacted by nearby spring flow, and surface water and subirrigation (Figures 7 and 8). Spatial analysis of the data revealed that areas with low vegetation cover (EVI <0.2) and low ET_g contribute to the majority of ET_g volume (67-74%) due to large contributing areas (87-93% of total phreatophyte areas).

TABLE 6. ET_g Mean Rates and Total Volumes (with prediction ranges) Estimated for Water Year 2006 in Phreatophyte Areas of White River Valley (WRV), Spring Valley (SPV), Dry Valley (DV), and Red Rock Valley (RRV).

Basin	Image Date	Landsat Path/Row	Area (km^2)	ET_o (m/yr)	PPT (m/yr)	ET_g (m/yr)	Pred. Int. (m/yr)	ET_g (Mm^3)	Pred. Int. (Mm^3)
WRV	8/07/2006	40/33	728.97	1.148[1]	0.22[1]	0.13	0.05-0.2	92.32	39-150
SPV	8/16/2006	39/33	740.50	1.296[2]	0.21[2]	0.14	0.06-0.22	99.95	45-165
DV	7/11/2006	43/32	9.00	1.192[3]	0.35[3]	0.18	0.1-0.25	1.62	1-2.3
RRV	7/11/2006	43/32	9.21	1.192[3]	0.35[3]	0.20	0.12-0.28	1.91	1.2-2.6

[1]Reported total is measured mean from stations WRV-1 and WRV-2.
[2]Reported total is measured mean from stations SPV-1, SPV-2, and SPV-3.
[3]Reported total is from Washoe County ET_o station located in Red Rock Valley.

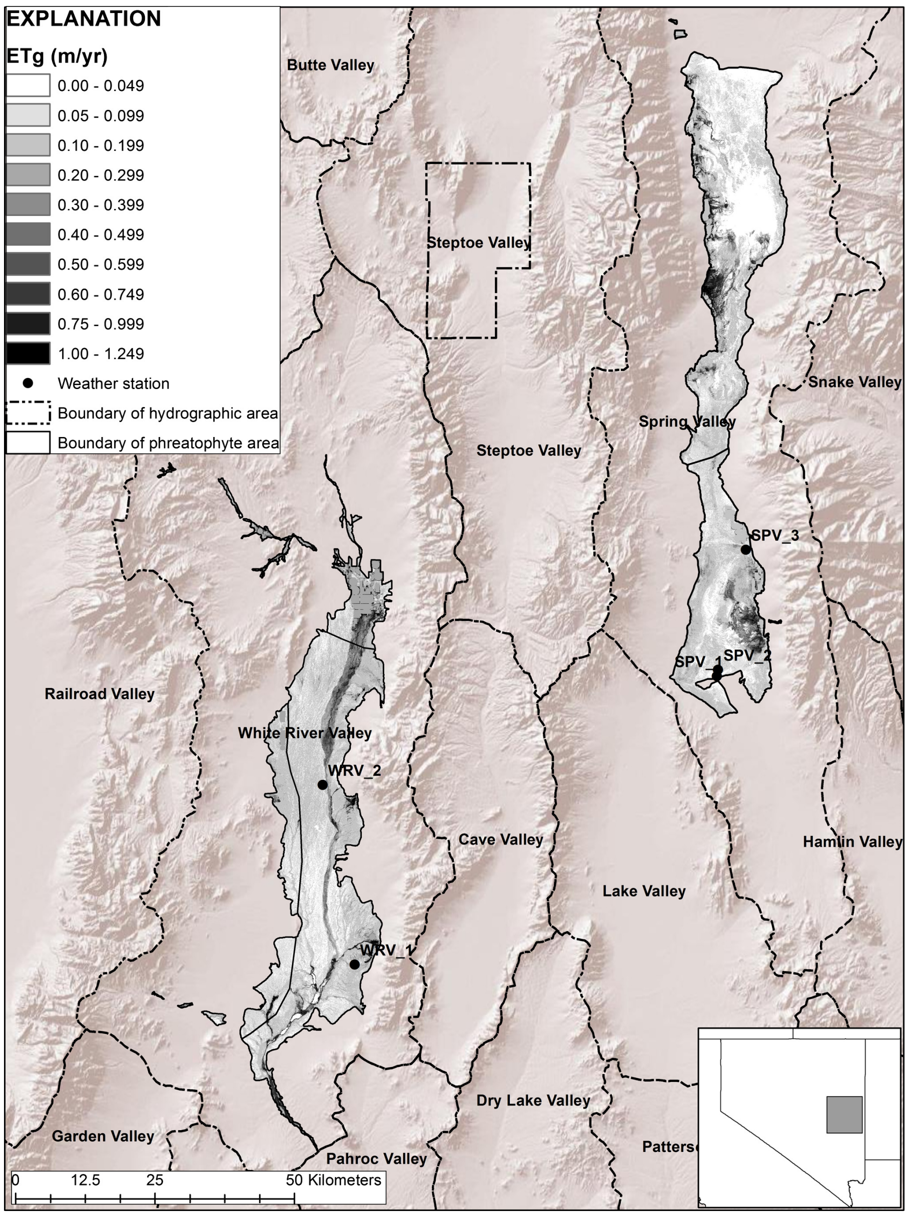

FIGURE 7. Map of First-Order Mean-Annual ET_g Rates (m/yr) from Phreatophyte Zones in Spring and White River Valleys, Eastern Nevada. Determined from Landsat data taken August 16, 2006 (Spring Valley, path 39 row 33) and August 7, 2006 (White River Valley, path 40 row 33).

Comparison with Previous Studies

To evaluate this approach with respect to previous approaches and ET_g estimates, ET_g estimates derived from this study were compared with those from previous studies in respective HAs (Table 7). Previous studies have applied a variety of methods to estimate ET_g, including remote sensing methods (Berger *et al.*, 2004; Moreo *et al.*, 2007; J.L. Huntington, "Estimates of Recharge and Discharge in Dry Valley Hydrographic Area", unpublished report, 2010), chloride mass balance for estimating groundwater recharge (Thomas and Albright, 2003), and extrapolation of flux tower estimates made from around the globe (L. Carpenter, "Applicants Estimate of Red Rock Valley Phreatophyte ET", unpublished report submitted to Nevada State Engineers Office, 2006). Mean ET_g volumes from previous estimates fall within 90% prediction intervals of this study for all four HAs (Figure 7), however, several estimates fall outside of the 90% confidence intervals. In Spring and White River Valley, mean ET_g volumes compare well with estimates provided by Moreo *et al.* (2007) and Zhu *et al.* (2007), who employed remote sensing and a Monte Carlo simulation to derive ET_g. Previous estimates fall below the lower 90% prediction interval for Dry and Red Rock Valley. These estimates

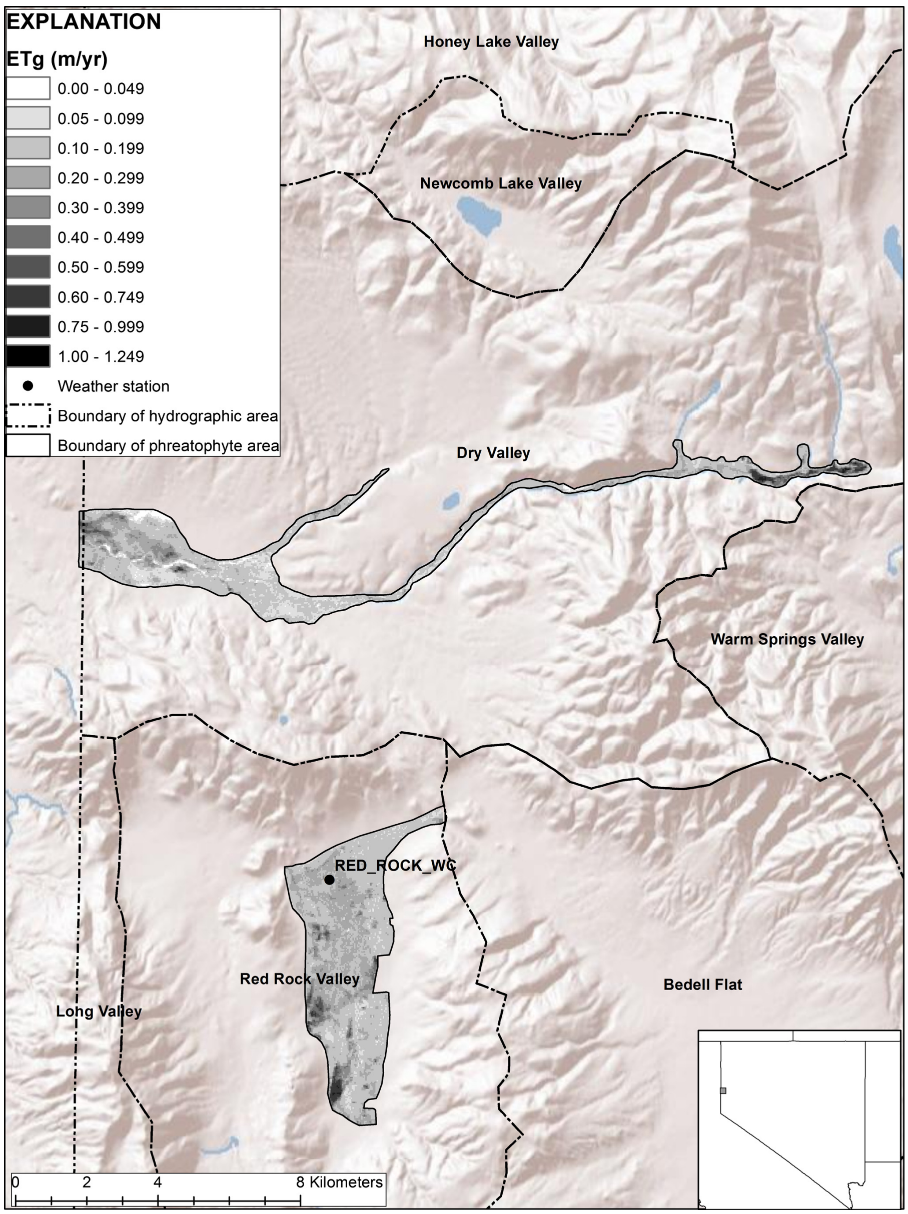

FIGURE 8. Map of First-Order Mean-Annual ET_g Rates (m/yr) for Phreatophyte Zones in Dry and Red Rock Valleys, Northwestern Nevada. Determined from Landsat data taken July 11, 2006 (path 43 row 32).

TABLE 7. Comparison of Annual ET_g Discharge Estimates (in Mm^3) for Spring Valley (SPV), White River Valley (WRV), Dry Valley (DV), and Red Rock Valley (RRV) from This and Previous Studies.

HA	Current Study	USGS	SNWA	NSEO	DRI	Zhu *et al.* (2007)	USGS Recon.	Other
SPV	99.95	93.27[1]	128.78[3]	103.74[4]		92.47	86.34[8]	111.01[11]
WRV	92.32	94.61[1]			98.68[6]	93.51	45.64[9]	
DV	1.62	0.79-0.98[2]			1.73[7]		0.1[10]	1.24-2.16[12]
RRV	1.91			0.99-2.47[5]			0.78[10]	2.5[13]

Notes: DRI, Desert Research Institute; NSEO, Nevada State Engineer's Office; SNWA, Southern Nevada Water Authority; USGS, U.S. Geological Survey.
[1]Welch *et al.* (2007). Estimate includes 2.4 Mm^3 from playa discharge for SPV.
[2]Berger *et al.* (2004).
[3]2006 values reported by Southern Nevada Water Authority (2011). Estimate includes 1.48 Mm^3 from playa discharge.
[4]Nevada State Engineers (2012) ruling #6164. Estimate includes 1.48 Mm^3 from playa discharge.
[5]Nevada State Engineers (2006) ruling #5816.
[6]Thomas *et al.* (2001).
[7]Thomas and Albright (2003).
[8]Rush and Kazmi (1965).
[9]Eakin (1966).
[10]Rush and Glancy (1967).
[11]Nichols (2000).
[12]J. L. Huntington, "Review and Analysis of Recharge and Discharge Estimates for Dry Valley, Washoe County, Nevada", unpublished report for United Management Corporation, 2010.
[13]Huffman and Carpenter, Inc., "Evapotranspiration Study – Utilizing Land Use Classification and Remote Sensing Methodologies for the Redrock Watershed (Basin 99), Washoe County, Nevada", unpublished report for Red Rock Valley Ranch, LLC, 2007.

were derived from early studies (Lee, 1912; White, 1932; Young and Blaney, 1942) and applied by Rush and Glancy (1967) in which ET_g was estimated at 0.09 m/yr, roughly half of the estimated rate from this work. In addition, phreatophyte areas estimated from Rush and Glancy (1967) were significantly smaller for Dry Valley than that estimated more recently using remote sensing methods (Berger *et al.*, 2004). Confidence intervals shown in Figure 9 have a fairly small range, and it is argued that these confidence intervals are a better representation of the model's uncertainty than the prediction intervals because the regression equation is meant to represent the mean behavior of the ET*-EVI data which are used to calculate ET_g. For estimation of the mean ET_g in a phreatophyte area using Equation (11), the confidence intervals should be used to describe the uncertainty in the model estimate.

DISCUSSION AND CONCLUSIONS

Methods for estimating mean-annual ET_g developed and applied in this study are not without uncertainties. Generally, uncertainties associated with estimates of ET_a and ET_g using methods described in this study can be broadly classified as errors in measurement and errors in scaling. EBC error is a major source of measurement error that needs to be addressed further in ET studies. With the advancement of instrumentation such as four-way net radiometers to

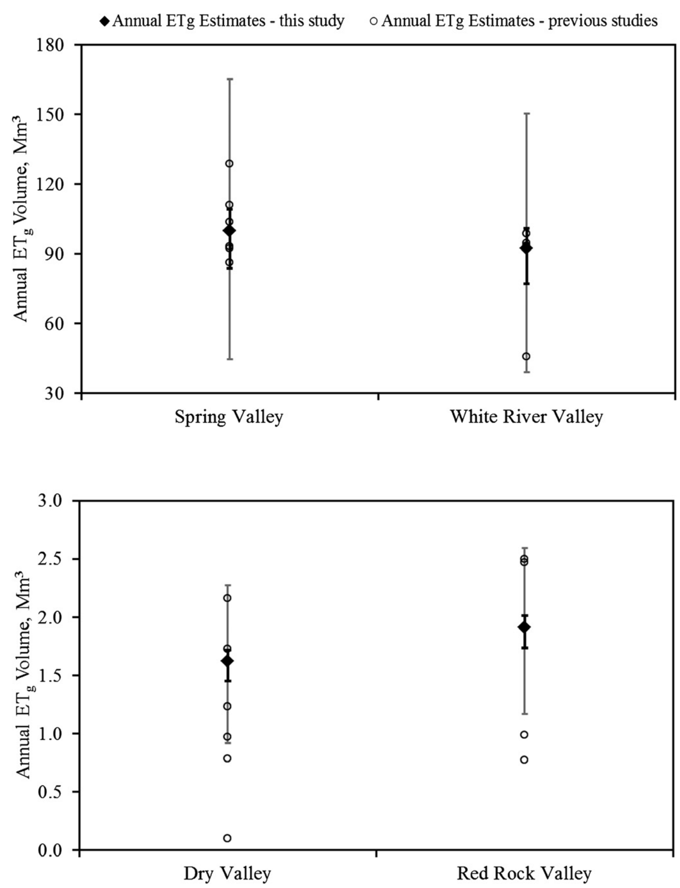

FIGURE 9. Estimates of Mean-Annual ET_g Volume (Mm^3) by Hydrographic Area in This Study (black diamonds) and Previous Studies (open circles). Black bars represent calculated uncertainty of mean value (90% confidence interval), gray bars represent 90% prediction intervals.

estimate R_n, heated-needle probes to directly calculate soil heat capacity and thermal conductivity, use of at least 6-10 soil heat flux plates and many sets of thermocouples at depth to accurately estimate G and heat storage, and use of multiple turbulent flux approaches used in combination such as combined BR-EC stations, the EBC problem can be better solved in the future to more accurately assess measurement error. Scaling error can arise from soil background noise in VI signals, nonphreatophyte VI response with-in phreatophyte groundwater discharge areas (e.g., from cheat grass), and the impact of precipitation on phreatophyte greenness and soil noise. Typically, money spent on estimating ET (i.e., BR, EC, remote sensing, etc.) can range from tens to hundreds of thousands of dollars. However, inaccurate estimates of precipitation derived from tipping buckets are often used to calculate ET_g from expensive and state-of-the-art estimates of ET_a. Installation of multiple, accurate precipitation gauges that account for possible under catch would greatly improve our ability to accurately estimate and upscale ET_g to larger spatial scales with more confidence.

This work builds on previous remote sensing of ET work in phreatophyte environments by developing a transferable function to estimate ET_g from phreatophytes using a fairly standard atmospheric correction algorithm and VI. The main advantages of this method are that it: (1) is fairly robust and simple to apply as long as annual ET_o and PPT data are available in the area of interest, (2) uses Landsat 5 TM data which are available at no cost and cover large areas, (3) is based on measurements of ET_a, ET_o, and PPT from a wide range of phreatophyte vegetation types and climates in the Great Basin, and (4) is scaled by ET_o and PPT representative of the HA of interest. Prediction and confidence intervals about the mean ET* will allow water resource modelers and managers to evaluate if independent groundwater discharge estimates are "believable" based on previous measurements of ET_g used to develop the regressions presented in this study. This approach will assist local, state, and federal agencies to independently evaluate expert witness reports of ET_g, along with providing new first-order estimates of ET_g with associated uncertainty.

ACKNOWLEDGMENTS

This project was funded by the U.S. Bureau of Reclamation Nevada Water Resources Evaluation Program in collaboration with the Nevada State Engineer's Office, funded by a grant under Public Law 109-103, Section 208(a), Cooperative Agreement 06FC204044. The authors wish to acknowledge the U.S. Geological Survey for supplying BR and EC data from stations in Carson Valley, Walker River Valley, White River Valley, Spring Valley, Snake Valley, Oasis Valley, and the lower Colorado River flow system as well as Jay Arnone and Richard Jasoni at Desert Research Institute for the EC data from Spring Valley. The comments and corrections provided by the reviewers were extremely valuable and much appreciated.

LITERATURE CITED

Allander, K.K., J.L. Smith, and M.J. Johnson, 2009. Evapotranspiration from the Lower Walker River Basin, West-Central Nevada, Water Years 2005-07. U.S. Geological Survey Scientific Investigations Report 2009-5079, 62 pp. http://pubs.usgs.gov/sir/2009/5079/.

Allen, R.G., L.S. Pereira, T.A. Howell, and M.E. Jensen, 2011. Evapotranspiration Information Reporting: I. Factors Governing Measurement Accuracy. Agricultural Water Management 98:899-920, doi: 10.1016/j.agwat.2010.12.015.

Allen, R.G., M. Tasumi, and R. Trezza, 2007. Satellite-Based Energy Balance for Mapping Evapotranspiration with Internalized Calibration (METRIC) – Model. Journal of Irrigation and Drainage Engineering 133(4):380-394, doi: 10.1061/(ASCE)0733-9437(2007) 133:4(380).

Allen, R.G., I.A. Walter, R.L. Elliott, T.A. Howell, D. Itenfisu, M.E. Jensen, and R.L. Snyder (Editors), 2005. The ASCE Standardized Reference Evapotranspiration Equation. American Society of Civil Engineers, Reston, Virginia.

Arnone, J., R. Jasoni, J. Larsen, L. Fenstermaker, G. Wolfahrt, C. Kraftt, B. Lyles, J. Healey, M. Young, and J. Thomas, 2009. Variable Evapotranspiration Water Losses from Lowland Agricultural and Native Shrubland Ecosystems in the Great Basin of Nevada. DRI Publication Number 655.7520.

Beamer, J.P., 2011. Estimation of Annual Groundwater Evapotranspiration from Phreatophyte Vegetation in the Great Basin Using Remotely Sensed Vegetation Indices and Ground Based Flux Tower Measurements. M.S. Thesis, University of Nevada, Reno, Nevada.

Berger, D.L., D.K. Maurer, T.J. Lopes, and K.J. Halford, 2004. Estimates of Natural Groundwater Discharge and Characterization of Water Quality in Dry Valley, Washoe County, West-Central Nevada, 2002-2003. U.S. Geological Survey Scientific Investigations Report 2004-5155, 46 pp. http://pubs.usgs.gov/sir/2004/5155/.

Blanken, P.D., T.A. Black, P.C. Yang, H.H. Neumann, Z. Nesic, R. Staebler, G. den Hartog, M.D. Novak, and X. Lee, 1997. Energy Balance and Canopy Conductance of a Boreal Aspen Forest: Partitioning Overstory and Understory Components. Journal of Geophysical Research 102(D24):28915-28927, doi: 10.1029/97JD00193.

Bowen, I.S., 1926. The Ratio of Heat Losses by Conduction and by Evaporation by Any Water Surface. Physics Review 27:779-787.

DeMeo, G.A., J.L. Smith, N.A. Damar, and J. Darnell, 2008. Quantifying Groundwater and Surface-Water Discharge from Evapotranspiration Processes in 12 Hydrographic Areas of the Colorado Regional Groundwater Flow System, Nevada, Utah, and Arizona. U.S. Geological Survey Scientific Investigations Report 2006-5145, 36 pp. http://pubs.usgs.gov/sir/2008/5116.

Devitt, D.A., L.F. Fenstermaker, M.H. Young, B. Conrad, M. Baghzouz, and B.M. Bird, 2011. Evapotranspiration of Mixed Shrub Communities in Phreatophytic Zones of the Great Basin Region of Nevada (USA). Ecohydrology 4(6):807-822, doi: 10.1002/eco.169.

Eakin, T.E., 1966. A Regional Interbasin Groundwater System in the White River Area, Southeastern Nevada. Water Resources Research 2(2):251-271.

Foken, T., 2008. The Energy Balance Closure Problem: An Overview. Ecological Applications 18(6):1351-1367.

Groeneveld, D.P., W.M. Baugh, J.S. Sanderson, and D.J. Cooper, 2007. Annual Groundwater Evapotranspiration Mapped from Single Satellite Scenes. Journal of Hydrology 344:146-156, doi: 10.1016/j.jhydrol.2007.07.002.

Halldin, S. and A. Lindroth, 1992. Errors in Net Radiometry, Comparison and Evaluation of Six Radiometer Designs. Journal of Atmospheric and Oceanic Technology 9(6):762-783.

Harrington, R., A. Steinwand, P. Hubbard, and D. Martin, 2004. Evapotranspiration from Groundwater Dependent Plant Communities: Comparison of Micrometeorological and Vegetation-Based Measurements. Report to the Inyo/Los Angeles Technical Group, September 15, 105 pp.

Helsel, D.R. and R.M. Hirsch, 2002. Statistical Methods in Water Resources. U.S. Geological Survey Techniques of Water Resources Investigation, Book 4, Chapter A3, 524 pp. http://water.usgs.gov/pubs/twri/twri4a3/.

Huntington, J.L., J. Szilagyi, S.W. Tyler, and G.M. Pohll, 2011. Evaluating the Complementary Relationship for Estimating Evapotranspiration from Arid Shrublands. Water Resources Research 47:W05533, doi: 10.1029/2010WR009874.

Kahler, D.M. and W. Brutsaert, 2006. Complementary Relationship between Daily Evaporation in the Environment and Pan Evaporation. Water Resources Research 42:W05413, doi: 10.1029/2005WR004541.

Kalma, J.D., T.R. McVicar, and M.F. McCabe, 2008. Estimating Land Surface Evaporation: A Review of Methods Using Remotely Sensed Surface Temperature Data. Surveys in Geophysics 29:421-469, doi: 10.1007/s10712-008-9037-z.

Laczniak, R.J., G.A. DeMeo, S.R. Reiner, J.L. Smith, and W.E. Nylund, 1999. Estimates of Groundwater Discharge as Determined from Measurements of Evapotranspiration, Ash Meadows Area, Nye County, Nevada. U.S. Geological Survey Water-Resources Investigation Report 99-4079, 70 pp. http://pubs.usgs.gov/wri/wri994079.

Lee, C.H., 1912. Water Resources of a Part of Owens Valley, California. U.S. Geological Survey Water Supply Paper 294, 135 pp.

Lee, X., 1998. On Micrometeorological Observations of Surface-Air Exchange over Tall Vegetation. Agricultural and Forest Meteorology 91:39-49, doi: 10.1016/S0168-1923(98)00071-9.

Liebethal, C. and T. Folken, 2007. Evaluation of Six Parameterization Approaches for the Ground Heat Flux. Theoretical and Applied Climatology 88:43-56, doi: 10.1007/s00704-005-0234-0.

Maurer, D.K., D.L. Berger, M.L. Tumbusch, and M.J. Johnson, 2005. Rates of Evapotranspiration, Recharge from Precipitation beneath Selected Areas of Native Vegetation, and Streamflow Gain and Loss in Carson Valley, Douglas County, Nevada, and Alpine County, California. U.S. Geological Survey Scientific Investigations Report 2005-5288, 70 pp. http://pubs.usgs.gov/sir/2005/5288.

Maxey, G.B. and T.E. Eakin, 1949. GroundWater in White River Valley, White Pine, Nye, and Lincoln Counties, Nevada. State of Nevada, Office of the State Engineer Water Resources Bulletin Number 8, 59 pp.

Meyers, T.P. and D.D. Baldocchi, 2005. Current Micrometeorological Flux Methodologies with Applications in Agriculture. *In*: Micrometeorology in Agricultural Systems (Agronomy), J.L. Hatfield (Editor). American Society of Agronomy Inc., Madison, Wisconsin, pp. 381-396.

Moreo, M.T., R.J. Laczniak, and D.I. Stannard, 2007. Evapotranspiration Rate Measurements of Vegetation Typical of Groundwater Discharge Areas in the Basin and Range Carbonate-Rock Aquifer System, White Pine County, Nevada, and Adjacent Areas in Nevada and Utah, September 2005-August 2006. U.S. Geological Survey Scientific Investigations Report 2007-5078, 36 pp. http://pubs.usgs.gov/sir/2007/5078.

Nagler, P.L., R.L. Scott, C. Westenburg, J.R. Cleverly, E.P. Glenn, and A.H. Huete, 2005. Evapotranspiration on Western U.S. Rivers Estimated Using the Enhanced Vegetation Index from MODIS and Data from Eddy Covariance and Bowen Ratio Flux Towers. Remote Sensing of Environment 97(3):337-351, doi: 10.1016/j.rse.2005.05.011.

Nevada State Engineer (The Office of the State Engineer of the State of Nevada), 2006. The Ruling (#5816) In the Matter of Applications 73960, 73961, 73963, 73965, 73966, and 74368 Filed to Appropriate or Change the Public Waters of an Underground Source within the Red Rock Valley Hydrographic Basin (99), Washoe County, Nevada, 51 pp.

Nevada State Engineer (The Office of the State Engineer of the State of Nevada), 2012. The Ruling (#6164) In the Matter of Applications 54003 through 54021, Inclusive, Filed to Appropriate the Underground Waters of the Spring Valley Hydrographic Basin (184), Lincoln and White Pine Counties, Nevada, 218 pp.

Nichols, W.D., 1993. Estimating Discharge of Shallow Groundwater by Transpiration from Greasewood in the Northern Great Basin. Water Resources Research 29(8):2771-2778, doi: 10.1029/93WR00930.

Nichols, W.D., 2000. Regional Groundwater Evapotranspiration and Groundwater Budgets, Great Basin, Nevada. U.S. Geological Survey Professional Paper 1628, 82 pp.

Qi, J., A. Chehbouni, A.R. Huete, Y.H. Kerr, and S. Sorooshian, 1994. A Modified Soil Adjusted Vegetation Index. Remote Sensing of Environment 48(2):119-126, doi: 10.1016/0034-4257(94)90134-1.

Reiner, S.R., R.J. Laczniak, G.A. DeMeo, J.L. Smith, P.E. Elliott, W.E. Nylund, and C.J. Fridrich, 2002. Groundwater Discharge Determined from Measurements of Evapotranspiration, Other Available Hydrologic Components, and Shallow Water-Level Changes, Oasis Valley, Nye County, Nevada. U.S. Geological Survey Water-Resources Investigations Report 01-4239, 65 pp. http://pubs.usgs.gov/wri/wri014239.

Rush, F.E. and P.A. Glancy, 1967. Water-Resources Appraisal of the Warm Springs-Lemmon Valley Area, Washoe County, Nevada. Nevada Department of Conservation and Natural Resources, Water Resources-Reconnaissance Report 43, Carson City, Nevada, 70 pp.

Rush, F.E. and S.A.T. Kazmi, 1965. Water Resources Appraisal of Spring Valley, White Pine and Lincoln Counties, Nevada. Nevada Department of Conservation and Natural Resources, Water Resources-Reconnaissance Report 33, Carson City, Nevada, 39 pp.

Senay, G.B., S. Leake, P.L. Nagler, G. Artan, J. Dickson, J.T. Cardova, and E.P. Glenn, 2011. Estimating Basin Scale Evapotranspiration (ET) by Water Balance and Remote Sensing Methods. Hydrological Processes, 25:4037-4049, doi: 10.1002/hyp.8379.

Smith, J.L., R.J. Laczniak, M.T. Moreo, and T.L. Welborn, 2007. Mapping Evapotranspiration Units in the Basin and Range Carbonate-Rock Aquifer System, White Pine County, Nevada, and Adjacent Areas in Nevada and Utah. U.S. Geological Survey Scientific Investigations Report 2007-5087, 31 pp. http://pubs.usgs.gov/sir/2007/5087/.

Southern Nevada Water Authority, 2011. Hydrology and Water Resources of Spring, Cave, Dry Lake, and Delamar Valley, Nevada and Vicinity, Southern Nevada Water Authority, Las Vegas, Nevada, 313 pp.

Steinwand, A.L., R.F. Harrington, and D. Or, 2006. Water Balance for Great Basin Phreatophytes Derived from Eddy-Covariance, Soil Water, and Water Table Measurements. Journal of Hydrology 329:595-605, doi: 10.1016/j.jhydrol.2006.03.013.

Tasumi, M., R.G. Allen, and R. Trezza, 2008. At-Surface Reflectance and Albedo from Satellite for Operational Calculation of Land Surface Energy Balance. Journal of Hydrologic Engineering 13(2):51-63, doi: 10.1061/(ASCE)1084-0699(2008)13:2(51).

Thomas, J.T. and W.H. Albright, 2003. Estimated Recharge to Dry Valley, Northeastern Nevada Using the Chloride Mass Balance Method. Desert Research Institute. DRI Publication Number 41191, 25 pp.

Thomas, J.T., S.C. Calhoun, and W.B. Apambire, 2001. A Deuterium Mass-Balance Interpretation of Groundwater Sources and Flows in Southeastern Nevada. Desert Research Institute. DRI Publication Number 41169, 46 pp.

Twine, T.E., W.P. Kustas, J.M. Norman, D.R. Cook, P.R. Houser, T.P. Meyers, J.H. Prueger, P.J. Starks, and M.L. Wesely, 2000. Correcting Eddy-Covariance Flux Underestimates over a Grassland. Agricultural and Forestry Meteorology 103(3):279-300, doi: 10.1016/S0168-1923(00)00123-4.

Welborn, T.L. and M.T. Moreo, 2007. Irrigated acreage within the Basin and Range Carbonate-Rock Aquifer System, White Pine County, Nevada, and Adjacent Areas in Nevada and Utah. U.S. Geological Survey Data Series 273, 18 pp.

Welch, A.H., D.J. Bright, and L.A. Knochenmus, 2007. Water Resources of the Basin and Range Carbonate-Rock Aquifer System, White Pine County, Nevada, and Adjacent Areas in Nevada and Utah. U.S. Geological Survey Scientific Investigations Report 2007-5261, 97 pp. http://pubs.usgs.gov/sir/2007/5261.

White, W.N., 1932. A Method of Estimating Groundwater Supplies Based on Discharge by Plants and Evaporation from Soils – Results from Investigations in Escalante Valley, Utah. U.S. Geological Survey Water-Supply Paper 659, 105 pp.

Young, A.A. and H.F. Blaney, 1942. Use of Water by Native Vegetation: California Department of Public Works, Division of Water Resources Bulletin 50, 160 pp.

Zhu, J., M.H. Young, and M.E. Cablk, 2007. Uncertainty Analysis of Estimates of Groundwater Discharge by Evapotranspiration for the BARCAS Study Area. Desert Research Institute. DRI Publication Number 41234, 20 pp.